Magnetochiral nonreciprocity of volume spin wave propagation in chiral-lattice ferromagnets

S. Seki,[1,2] Y. Okamura,[3] K. Kondou,[1] K. Shibata,[3] M. Kubota,[1,4,*] R. Takagi,[1] F. Kagawa,[1]
M. Kawasaki,[1,3] G. Tatara,[1] Y. Otani,[1,5] and Y. Tokura[1,3]

[1]*RIKEN Center for Emergent Matter Science (CEMS), Wako 351-0198, Japan*
[2]*PRESTO, Japan Science and Technology Agency (JST), Tokyo 113-8656, Japan*
[3]*Department of Applied Physics and Quantum Phase Electronics Center (QPEC), University of Tokyo, Tokyo 113-8656, Japan*
[4]*Research and Development Headquarters, ROHM Co., Ltd., Kyoto 615-8585, Japan*
[5]*Institute for Solid State Physics, University of Tokyo, Kashiwa 277-8581, Japan*

(Received 26 July 2015; revised manuscript received 8 May 2016; published 16 June 2016)

In magnetic materials with chiral crystal structure, it has been predicted that quasiparticle flows propagating parallel and antiparallel to the external magnetic field can show different propagating character, with its sign of nonreciprocity dependent on the chirality of the underlying bulk crystal lattice. This unique phenomenon, termed *magnetochiral* nonreciprocity, has previously been demonstrated for the propagating light and conduction electrons but seldom for other quasiparticles. In this study, we report the experimental observation of *magnetochiral* nonreciprocity of propagating magnons for a chiral-lattice ferromagnet Cu_2OSeO_3 by employing the spin wave spectroscopy. We found that the sign of nonreciprocity is reversed for the opposite chirality of crystal, and also directly identified the wave-number-linear term in the spin wave dispersion associated with the Dzyaloshinskii-Moriya (DM) interaction as the origin of observed nonreciprocity. Our present results pave a route for the design of efficient spin wave diode based on the bulk crystallographic symmetry breaking and also offer a unique method to evaluate the magnitude of DM interaction in chiral-lattice bulk compounds.

DOI: 10.1103/PhysRevB.93.235131

I. INTRODUCTION

The interplay between crystallographic chirality and magnetism has recently attracted much attention as the source of rich emergent phenomena [1,2]. For example, in ferromagnetic materials with chiral crystallographic lattice, the appearance of Dzyaloshinskii-Moriya (DM) interaction often stabilizes magnetic skyrmion, i.e., vortexlike swirling spin texture with particle nature [3–8]. In general, the size of skyrmion a_{Sk} is determined by the ratio between the magnitudes of DM interaction D and ferromagnetic exchange interaction J (i.e., $a_{\mathrm{Sk}} \sim J/D$), with the upper limit of skyrmion size on the order of 100 nm [9]. Magnetic skyrmion is now considered as a promising candidate of efficient information carriers for high-density magnetic storage device, where the appropriate evaluation of the magnitude of DM interaction is the key for the search of new materials with smaller size of skyrmions.

On the other hand, the chiral-lattice ferromagnets are also predicted to host *magnetochiral* nonreciprocity for quasiparticle flow of various kinds [10,11]. When the quasiparticle flow with the wave vector $\vec{k}$ propagates along the magnetic field $\vec{H}$ in the chiral-lattice ferromagnets, the relevant response function is described as

$$A(\vec{k},\vec{H},\sigma) = A_0 + \sigma[\mathrm{sgn}(\vec{k}\cdot\vec{H})]A_{\mathrm{MCh}}. \quad (1)$$

Here, σ is defined to take the value $+1$ or -1 depending on the chirality (D or L, corresponding to the right or left handedness) of underlying crystal structure, and A_0 and A_{MCh} represent the conventional and *magnetochiral* terms in the response function, respectively. This means that the quasiparticle flows propagating parallel and antiparallel to $\vec{H}$ show different propagation character in the chiral-lattice compound, where the sign of nonreciprocity should be reversed by employing the opposite chirality of crystal or opposite direction of $\vec{H}$. Such *magnetochiral* nonreciprocity has been predicted based on the symmetry arguments [10,11], and later experimentally established by Rikken *et al.* for propagating light (i.e., *magnetochiral* directional dichroism) [12–15] and conduction electrons (i.e., electrical *magnetochiral* anisotropy) [16,17] but still not for other quasiparticles.

In ferromagnetic materials, the most fundamental elementary excitation is magnon or spin wave, representing the propagating spin precession. Recently, spin wave attracts revived interest as the carrier of spin current (i.e., flow of spin angular momentum) in insulators, which can be the energy-efficient alternative of charge current without the loss of Joule heating [18–21]. Under the $\vec{k} \parallel \vec{H}$ configuration, the spin wave at the $k \to 0$ limit is called volume spin wave, which is known to propagate through the entire volume of the sample [22–24]. While this mode should not show any nonreciprocity in the centrosymmetric ferromagnets, *magnetochiral* nonreciprocity of volume spin wave propagation has been theoretically predicted for chiral-lattice ferromagnets, due to the k-linear term in the spin wave dispersion originating from DM interaction [25–27]. However, such *magnetochiral* nonreciprocity of propagating magnon has remained yet to be established experimentally, partly because the expected magnitude of asymmetry in the dispersion relationship is too small to be detected by the conventional inelastic neutron diffraction technique due to the resolution limit [28,29]. Very recently, the nonreciprocal propagation character of magnon has been investigated in a noncentrosymmetric ferromagnet $LiFe_5O_8$, although its relationship with crystallographic chirality is unclear and the emergence of higher-order modes (possibly due to the large sample thickness and multiple

*Present Address: Technology and Business Development Unit, Murata Manufacturing Co., Ltd., Nagaokakyo, Kyoto 617-8555, Japan.

reflection of spin wave) prevented the clear identification of k-linear nature of spin wave dispersion [30]. To establish the *magnetochiral* nonreciprocity of propagating magnon, (1) the coupling between the crystallographic chirality and the sign of nonreciprocity, as well as (2) the existence of the k-linear term in the spin wave dispersion, must be directly demonstrated for chiral-lattice ferromagnets.

In this paper, we report the experimental observation of *magnetochiral* nonreciprocity of magnon (or volume spin wave) propagation for a chiral-lattice ferromagnet Cu_2OSeO_3. By employing the spin wave spectroscopy technique accompanied with the vector analysis [31,32], we found that the spin waves propagating parallel and antiparallel to the magnetic field show different propagation character in terms of eigenfrequency, amplitude, and group velocity. Importantly, the sign of nonreciprocity turns out to be reversed by employing the opposite chirality of crystal or opposite direction of magnetic field, which unambiguously proves the *magnetochiral* nature of the observed nonreciprocity. By analyzing the experimentally obtained spin wave dispersion relationship, the k-linear term due to DM interaction has been directly detected as the origin of observed nonreciprocity. Our present results suggest that the design of efficient diode for volume spin wave is possible based on the bulk crystallographic symmetry breaking, and also offer a unique experimental method to evaluate the magnitude of DM interaction in the chiral-lattice bulk compounds that may be useful for the search of new candidate materials hosting magnetic skyrmions.

II. MATERIAL AND EXPERIMENTAL METHODS

Our target material Cu_2OSeO_3 is a ferromagnetic insulator, characterized by the chiral crystal structure with the cubic space group $P2_13$ as shown in Fig. 1(a) [33–35]. The magnetism is dominated by the Cu^{2+} ion with $S = 1/2$, and the detailed H-T (temperature) phase diagram is provided in Ref. [36]. For $H \to 0$, the helical spin order appears below magnetic transition temperature $T_c \sim 59$ K, where helical spins are confined within a plane normal to the external magnetic field. Above the critical magnitude of H, this helical spin state is replaced by the the uniform collinear ferromagnetic state. Cu_2OSeO_3 is also known as the first-discovered insulating material to host magnetic skyrmion, which appears for the narrow temperature region ($T_c > T > 56$ K) just below T_c [36–38]. In this study, we mainly investigate the spin wave propagation character in the uniform collinear ferromagnetic state.

Single crystals of Cu_2OSeO_3 were grown by the chemical vapor transport method [39]. The chirality of each Cu_2OSeO_3 crystal (D or L) was checked by measuring the sign of natural optical activity at light wavelength 1310 nm. Every piece of crystal shows optical rotation angle 16°/mm, and its single-domain nature is confirmed by the observation under polarized-light microscope.

The basic concept of the spin wave spectroscopy [31,32] as well as the employed device structure is summarized in Figs. 1(b) and 1(c). A pair of Au coplanar wave guides (ports 1 and 2) were fabricated on the oxidized silicon substrate, and the plate-shaped Cu_2OSeO_3 single crystal with the appropriate chirality was placed across them with W

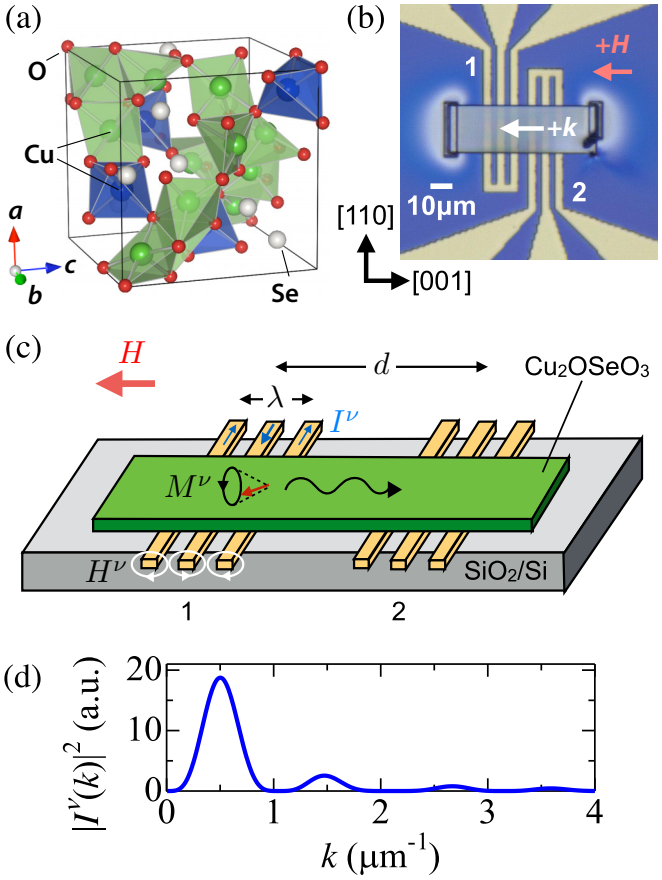

FIG. 1. (a) Crystal structure of Cu_2OSeO_3 characterized by the chiral cubic space group $P2_13$. (b) The optical microscope image and (c) schematic illustration of the device structure used for spin wave spectroscopy. In (b), the directions for positive sign of $\vec{H}$ and $\vec{k}$ are also indicated. See the main text for the detail. (d) Wave number distribution of excitation current $\tilde{I}^\nu(k)$, obtained by the Fourier transform of the wave guide pattern with $\lambda = 12$ μm.

deposition at both edges of the crystal using the focused ion beam (FIB) microfabrication technique. When the oscillating electric current I^ν of gigahertz frequency ν is injected into one of the waveguides, I^ν generates oscillating magnetic field H^ν and excites spin wave (i.e., coherent magnetization oscillation M^ν) in the Cu_2OSeO_3 sample. The propagating spin wave causes an additional magnetic flux on the wave guides and induces the oscillating electric voltage V^ν following Faraday's law. By measuring the spectrum of complex inductance $L_{nm}(\nu)$ as defined by $V_n^\nu = \sum_m L_{nm}(\nu)\frac{dI_m^\nu}{dt}$ (with m and n representing the port numbers used for the excitation and detection, respectively) with the vector network analyzer (VNA), we can evaluate both magnitude and phase of propagating spin wave. The spin wave contribution to the inductance spectrum $\Delta L_{nm}(\nu) = L_{nm}(\nu) - L_{nm}^{\rm ref}(\nu)$ is derived by the subtraction of the common background $L_{nm}^{\rm ref}(\nu)$ from the raw data $L_{nm}(\nu)$. Here, $L_{nm}(\nu)$ taken at $H = 2650$ Oe is adopted as the reference spectrum $L_{nm}^{\rm ref}(\nu)$, where the magnetic resonance is absent within our target frequency range from 2 GHz to 7 GHz. The wave number k of excited spin wave is determined by the spatial periodicity λ ($= 12$ μm) of the waveguide pattern and the associated current density $I^\nu(x)$ [31,32]. Its Fourier

transform $|\tilde{I}^{v}(k)|^2$ has the main peak at $k_p = 0.50\ \mu\text{m}^{-1}$ with the full width at half maximum (FWHM) of $\delta k = 0.37\ \mu\text{m}^{-1}$ as plotted in Fig. 1(d), satisfying the relationship $k_p \sim 2\pi/\lambda$ (see Appendix A for the detail). To investigate the property of volume spin wave mode, the $H \parallel k \parallel [001]$ configuration is always adopted here. In the centrosymmetric materials, this mode should not show any nonreciprocal propagation nature [22–24].

III. RESULTS

First, we have investigated the nature of spin wave in the uniform collinear ferromagnetic state with saturated magnetization. Figures 2(a) and 2(b) indicate the real and imaginary part of ΔL_{11} and ΔL_{21} spectra measured at +740 Oe, i.e., in the collinear ferromagnetic state, for the D chirality of the Cu_2OSeO_3 crystal. The self-inductance ΔL_{11} represents the efficiency of the local spin wave excitation, and the ferromagnetic resonance characterized by Lorentzian shape of spectrum can be identified at 3.2 GHz. In contrast, the mutual-inductance ΔL_{21} reflects the propagation character of spin wave between the two wave guides, and the finite oscillating signal can be detected around the same resonance frequency. Hereafter, we focus on the comparison between ΔL_{21} and ΔL_{12}, each of which stands for the propagating spin wave characterized by the wave vector $+k$ and $-k$, respectively. To interpret the data more intuitively, the spectra of $|\Delta L_{nm}|$ and ϕ as defined with $\Delta L_{nm} = \text{Re}[\Delta L_{nm}] + i\ \text{Im}[\Delta L_{nm}] = |\Delta L_{nm}| \exp[i\phi]$ are plotted in Figs. 2(c) and 2(d). $|\Delta L_{21}|$ and $|\Delta L_{12}|$ express the magnitude of spin wave after the propagation along the positive and negative directions, and both spectra show a peak structure. Notably, the peak frequency ν_p as well as the peak intensity $|\Delta L^{p}_{nm}|$ are clearly different between $\pm k$. On the other hand, ϕ represents the phase delay of spin wave for a transmission between the two wave guides separated by the distance $d(= 20\ \mu\text{m})$, and will satisfy the relationship $\phi = kd$ when a single spin wave mode is assumed [31,32]. This means that the ϕ spectrum directly reflects the spin wave dispersion relationship, and its slope gives the group velocity $v_g = \frac{\partial\omega}{\partial k} = 2\pi d(\frac{\partial\phi}{\partial\nu})^{-1}$. The clear difference in the ϕ slope between ΔL_{21} and ΔL_{12} indicates that v_g of spin wave is not equal between $\pm k$. The above results establish that the propagation character of spin wave in this configuration is nonreciprocal, from both aspects of magnitude and group velocity.

To reveal the origin of nonreciprocity, the measurements of $\text{Im}[\Delta L_{21}]$ and $\text{Im}[\Delta L_{12}]$ were performed with various combinations of the magnetic field direction ($H = \pm 740$ Oe) and crystallographic chirality (D and L) for Cu_2OSeO_3 [Figs. 2(e)–2(h)]. Figure 2(e) shows the data for the D crystal at +740 Oe. The spectra of $\text{Im}[\Delta L_{21}]$ and $\text{Im}[\Delta L_{12}]$ are characterized by the signal oscillating with different period and magnitude, in agreement with the feature observed for $|\Delta L_{nm}|$ and ϕ. For the opposite sign of applied H [Fig. 2(f)], the spectral shapes for $\text{Im}[\Delta L_{21}]$ and $\text{Im}[\Delta L_{12}]$ (i.e., the sign of nonreciprocity) are reversed. More importantly, the employment of opposite chirality of crystal (i.e., L crystal) also reverses the sign of nonreciprocity [Figs. 2(g) and 2(h)]. Here,

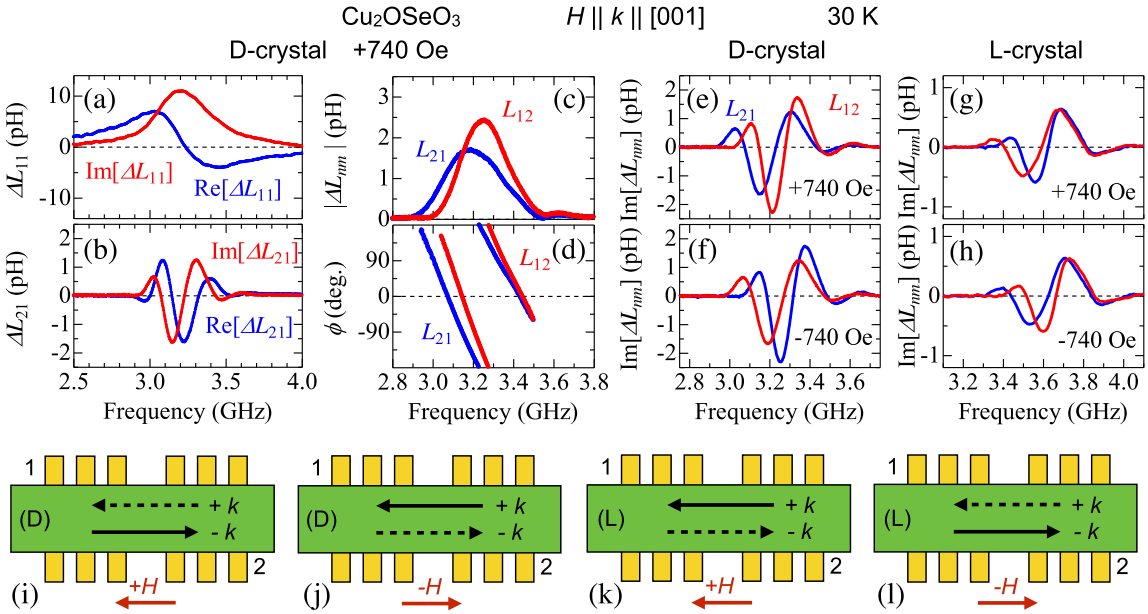

FIG. 2. (a)–(h) Spin wave contribution to inductance spectrum $\Delta L_{nm} = \text{Re}[\Delta L_{nm}] + i\ \text{Im}[\Delta L_{nm}] = |\Delta L_{nm}| \exp[i\phi]$, measured for the D or L chirality of Cu_2OSeO_3 single crystal with the $H \parallel k \parallel [001]$ configuration at 30 K. All the data are taken at the uniform collinear ferromagnetic state. (a) and (b) Real and imaginary part of self inductance ΔL_{11} and mutual inductance ΔL_{21} measured for the D crystal at $H = +740$ Oe. For the same configuration, (c) magnitude $|\Delta L_{nm}|$ and (d) phase ϕ of ΔL_{21} and ΔL_{12} are also plotted. (e)–(h) Imaginary part of ΔL_{21} and ΔL_{12}, measured with various combinations of magnetic field direction ($H = \pm 740$ Oe) and crystallographic chirality (D or L). Note that the deviation of the overall signal magnitude and resonance frequency between D and L crystal is due to the slight difference in their sample size and associated demagnetizing field. The corresponding experimental configurations as well as the expected sign of nonreciprocity are summarized in (i)–(l). Here, the spin wave characterized by the wave vector $+k$ ($-k$) contributes to ΔL_{21} (ΔL_{12}), and the solid and dashed arrows represent the different propagation characters.

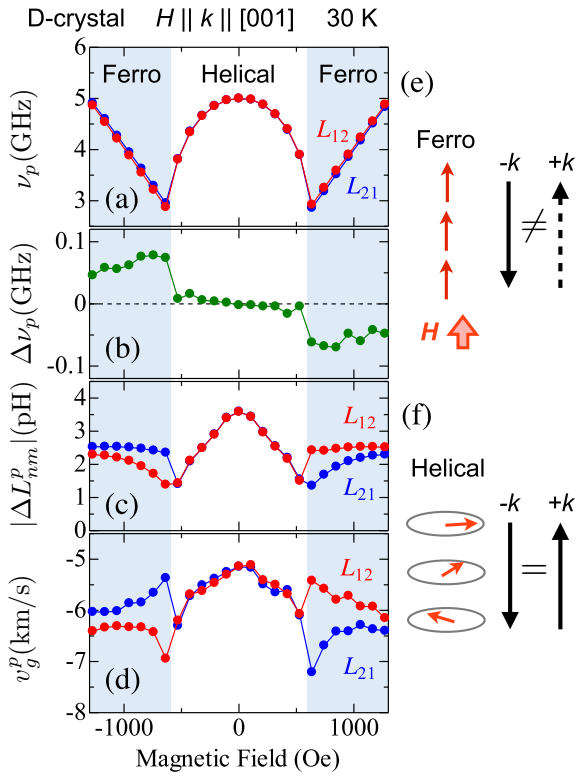

FIG. 3. Magnetic field dependence of spin wave nonreciprocity between ΔL_{21} and ΔL_{12} (i.e., $+k$ and $-k$), measured for the D crystal of Cu_2OSeO_3 with the $H \parallel k \parallel [001]$ configuration at 30 K. (a) and (b) indicate the magnetic resonance frequencies ν_p giving the peak value of $|\Delta L_{nm}|$, and their difference between $\pm k$ [i.e., $\Delta\nu_p = \nu_p(+k) - \nu_p(-k)$], respectively. In (c) and (d), the corresponding peak value $|\Delta L^p_{nm}|$ and the group velocity v^p_g at the frequency ν_p are also plotted. (e) and (f) Schematic illustration of collinear ferromagnetic state and helical spin state, respectively. The nonreciprocal spin wave propagation between $\pm k$ appears only in the former spin state.

we have performed the same measurements for three different L crystals and three different D crystals (not shown), and the sign of nonreciprocity was confirmed to be always opposite between the former and the latter ones. In Figs. 2(i)–2(l), the symmetrically expected sign of *magnetochiral* nonreciprocity for each experimental configuration is summarized based on Eq. (1). These are in agreement with our experimental results, which proves that the observed nonreciprocity originates from the chirality of the underlying bulk crystallographic lattice.

Next, we investigated the magnetic field dependence of nonreciprocity. In Figs. 3(a) and 3(b), the peak frequency ν_p for $|\Delta L_{21}|$ and $|\Delta L_{12}|$ [defined as $\nu_p(+k)$ and $\nu_p(-k)$], as well as the difference between them [$\Delta\nu_p = \nu_p(+k) - \nu_p(-k)$], is plotted as a function of H. Cu_2OSeO_3 is known to host the helical spin order for $H = 0$ [Fig. 3(f)] [36–38], while it is replaced with the uniform collinear ferromagnetic order for $H > 600$ Oe [Fig. 3(e)]. The magnetic resonance frequency is gradually suppressed by H in the helical spin state, and then shows H-linear increase in the collinear ferromagnetic state. These behaviors are consistent with the previous reports [40–42]. Notably, the magnitude of nonreciprocity is essentially dependent on the underlying magnetic structure. While the relatively large shift of resonance frequency $\Delta\nu_p \sim 0.05$ GHz between $\pm k$ is always observed for the collinear ferromagnetic state, such a nonreciprocity suddenly vanishes upon the transition into the helical spin state. Similar behavior is also observed for the peak intensity $|\Delta L^p_{nm}|$ [Fig. 3(c)] and group velocity v^p_g [Fig. 3(d)] deduced at ν_p. For all these properties, clear nonreciprocity is observed only in the collinear ferromagnetic state. Note that ν_p, $|\Delta L^p_{nm}|$, and v^p_g basically reflect the frequency, magnitude, and group velocity of spin wave for $|k| = k_p$. Their sign of nonreciprocity is confirmed to reverse for H reversal.

According to Refs. [25–27,43], the magnetic Hamiltonian for the ferromagnets with chiral cubic lattice symmetry under the continuum approximation can be written as $\mathcal{H} = \int E d\vec{r}$ with energy density E given by

$$E = \frac{J}{2}(\nabla\vec{S})^2 - \sigma D\vec{S}\cdot[\nabla\times\vec{S}] - \frac{K}{2}\sum_i S_i^4 - \frac{\gamma\hbar}{V_0}\mu_0\vec{H}\cdot\vec{S}, \tag{2}$$

where J, D, and K describe the magnitude of ferromagnetic exchange, DM, and cubic anisotropy term, respectively. Note that D is defined to take positive value, and the sign of DM interaction is coupled with the crystallographic chirality σ because of the symmetry requirement [9,44–46]. $\vec{S}$ is dimensionless parameter representing the vector spin density. γ, μ_0, $h = 2\pi\hbar$, and V_0 are gyromagnetic ratio, vacuum magnetic permeability, Planck constant, and the volume of formula unit cell of Cu_2OSeO_3, respectively. For the $H \parallel k \parallel [001]$ configuration, the spin wave dispersion $\nu(k)$ for the uniform collinear ferromagnetic state [Fig. 3 (e)] is described as [26]

$$\nu = \sigma[\mathrm{sgn}(\vec{k}\cdot\vec{H})]\frac{2DSV_0|k|}{h} + \frac{C_{\mathrm{sym}}}{h} \tag{3}$$

with $C_{\mathrm{sym}} = JSV_0k^2 + 2KV_0S^3 + \gamma\hbar\mu_0H$ being even function of k. In the real sample, this dispersion is further modified by the additional contribution of the magnetic dipole-dipole interaction, especially for the $k \to 0$ region. When the infinitely wide plate-shaped sample with the thickness l is assumed and $H \parallel k \parallel [001]$ lies along the in-plane direction, Eq. (3) can be rewritten as [23,24,27]

$$\nu = \sigma[\mathrm{sgn}(\vec{k}\cdot\vec{H})]\frac{2DSV_0|k|}{h} + \frac{C_{\mathrm{sym}}}{h}\sqrt{\left(1 + \frac{\gamma\hbar\mu_0M_s}{C_{\mathrm{sym}}}\frac{(1-e^{-|k|l})}{|k|l}\right)}, \tag{4}$$

with M_s being the saturation magnetization. In Figs. 4(d) and 4(e), the spin wave dispersion calculated based on Eq. (4) with the material parameters estimated for Cu_2OSeO_3 is plotted. Equation (4) can be approximated by Eq. (3) except for the $k \to 0$ region and gives parabolic dispersion with its minimum at $|k| = D/J$. As k approaches zero, however, the contribution of magnetic dipole-dipole interaction gradually increases the spin wave frequency. It causes the negative group velocity for the $k \to 0$ region, and this mode can be considered as a kind of magnetostatic backward volume spin wave [23,24]. Note that the first and second term in Eq. (4) are odd and even functions of k, respectively, and thus only the former one proportional to σDk can contribute to the spin wave nonreciprocity. This

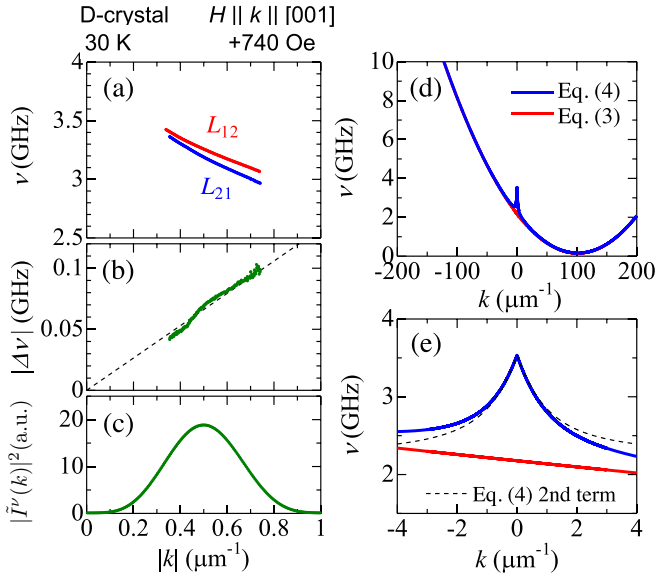

FIG. 4. (a) Spin wave dispersion for the D crystal of Cu_2OSeO_3 at $H = +740$ Oe (i.e., collinear ferromagnetic state), experimentally deduced by analyzing the ϕ spectrum in Fig. 2(d). The one obtained from ΔL_{21} (ΔL_{12}) corresponds to positive (negative) k value, and the frequency difference between $\pm k$ [i.e., $\Delta\nu(|k|) = \nu(+|k|) - \nu(-|k|)$] is also plotted in (b). (c) Wave number distribution of excitation current $\tilde{I}^{\nu}(k)$, obtained by the Fourier transform of the wave guide pattern. (d) and (e) Spin wave dispersions for the collinear ferromagnetic state calculated based on Eq. (4) or Eq. (3), the latter of which ignores the effect of magnetic dipole-dipole interaction. The black dashed line represents the contribution of the second term in Eq. (4). Here, the assumed material parameters are $l = 2$ μm, $D = 3.4 \times 10^{-4}$ J/m^2, $J = 3.4 \times 10^{-12}$ J/m, $K = 6.9 \times 10^3$ J/m^3, $\gamma/2\pi = 29$ GHz T^{-1}, $\mu_0 M_s = 0.12$ T, $\mu_0 H = 0.074$ T, $V_0 = 89$ Å^3, and $S = 0.44$. (See Appendix B for the detail.)

suggests that the observed nonreciprocity directly comes from the DM interaction, whose sign and magnitude reflect the chirality of the underlying crystallographic lattice through the relativistic spin-orbit interaction [9,44,45].

Experimentally, the above spin wave dispersion relationship can be partly reproduced by analyzing the ϕ spectrum [Fig. 2(d)]. Given that the frequency $\nu = \nu_p$ corresponds to the wave number $k = k_p$ and that the relationship $\phi = kd$ holds [31,32], the dispersion relationship can be determined by $k = [\phi(\nu) - \phi(\nu_p)]/d + k_p$. In Fig. 4(a), the spin wave dispersions $\nu(k)$ for the collinear ferromagnetic state [Fig. 3(e)] deduced from the ΔL_{21} and ΔL_{12} spectra [Figs. 2(c) and 2(d)] are plotted, each of which corresponds to the one for positive and negative k, respectively. The dispersion curves for positive and negative k show considerable deviation from each other, and their frequency shift $\Delta\nu(|k|) = \nu(+|k|) - \nu(-|k|)$ is plotted in Fig. 4(b). $\Delta\nu$ is found to be proportional to $|k|$, which is consistent with the relationship $\Delta\nu = 4DSV_0|k|/h$ expected from Eq. (4). Based on the observed frequency shift $\Delta\nu_p \sim 0.05$ GHz at $|k| = k_p$, we obtained $D \sim 4.2 \times 10^{-4}$ J/m^2. This is roughly in agreement with $D \sim 3.4 \times 10^{-4}$ J/m^2 estimated from H dependence of magnetic resonance frequency [41]. Such k-linear nature of frequency shift $\Delta\nu$ has also been confirmed by additional measurements with the different k_p value of the wave guide (See Appendix A for the detail). These results firmly establish that the observed spin wave nonreciprocity stems from the DM interaction associated with the chiral symmetry breaking by the bulk crystallographic lattice. Note that usually the inelastic neutron diffraction technique has been utilized as the method to determine the spin wave dispersion in bulk materials, while the experimental detection of such a magnitude of asymmetry (or corresponding frequency shift between $\pm k$) would be very difficult because of its resolution limit.

Lastly, we briefly discuss the origin of the observed disappearance of nonreciprocity in the helical spin state [Fig. 3(f)]. For the helical spin state under the magnetic Hamiltonian given by Eq. (2), it has been proposed that the Brillouin zone is folded back with the helical spin modulation period due to the expansion of magnetic unit cell [26,47,48]. Such a folding back of magnon branch should extinguish the asymmetry between $\pm k$, and therefore the nonreciprocity of spin wave propagation vanishes in the helical spin state.

IV. DISCUSSION AND CONCLUSION

In this study, we have experimentally observed *magnetochiral* nonreciprocity of volume spin wave propagation in a chiral-lattice ferromagnet Cu_2OSeO_3, by employing the spin wave spectroscopy technique. We have successfully demonstrated (1) the coupling between the crystallographic chirality and the sign of nonreciprocity and also directly detected (2) the existence of the k-linear term in the spin wave dispersion, which unambiguously proves that the observed nonreciprocity originates from the DM interaction associated with the chiral symmetry in the bulk crystallographic structure. This measurement procedure also enables the direct evaluation of DM interaction in the chiral-lattice bulk compound based on the shift of spin wave frequency between $\pm k$, and will contribute to the search for new candidate materials hosting magnetic skyrmions with smaller size.

Note that this *magnetochiral* nonreciprocity observed in the $H \parallel k$ setup is distinctive from the well-established nonreciprocity of surface spin wave, i.e., the $k \to 0$ spin wave mode in the $H \perp k$ setup that can propagate only at the surface of the sample [22–24,49]; the nonreciprocity of the latter case should be insensitive to the chirality of the underlying bulk crystal structure and rather originates from the polar symmetry breaking at the surface/interface of the sample (see Appendix C for the detail). Recently, the relevance of DM interaction has also been discussed for the latter case of surface/interface-driven nonreciprocity [50–52] through the spin-polarized electron energy loss spectroscopy [53] and Brillouin light scattering experiments [54,55], while such a DM contribution rapidly decays within a few nanometers apart from the surface [55]. Since the sign of structural polarity (and the resultant nonreciprocity of surface spin wave) is generally opposite between the top and bottom surfaces, this surface-driven nonreciprocity can also (partly) cancel out as the entire sample and spatially inhomogeneous excitation field must be employed to obtain a considerable amount of net nonreciprocity [56].

In contrast, the presently observed *magnetochiral* nonreciprocity is for the volume spin wave and originates from

the chiral symmetry breaking by the bulk crystal structure itself (rather than the surface). This provides the uniform DM interaction and rectification function throughout a single-component crystal of any shape and size in principle, which will be a unique advantage for the potential spin-wave diode functionality. Our present approach based on the bulk crystallographic symmetry breaking will offer a simple and promising route for the design of efficient volume spin wave diode, and highlight chiral-lattice ferromagnets as the source of novel spintronic function in terms of spin current as well as magnetic skyrmions.

More importantly, the present results demonstrate that the concept of *magnetochiral* nonreciprocity is applicable not only for the previously reported propagating light [12] and conduction electrons [16], but also for magnons. This contributes to the general understanding on the interplay between the crystallographic chirality and magnetism, and the further investigation of *magnetochiral* nonreciprocity for other quasiparticle flows will be interesting.

ACKNOWLEDGMENTS

The authors thank M. Mochizuki, T. Arima, N. Nagaosa, D. Morikawa, Y. Tokunaga, N. Kanazawa, Y. Nii, N. Ogawa, A. Kikkawa, and X. Z. Yu for enlightening discussions and experimental help. This work was partly supported by the Mitsubishi Foundation, Grants-In-Aid for Scientific Research (Grant Nos. 26610109, 15H05458, 16K13842, 25400344, 26103002, 26103006) from JSPS and the MEXT of Japan.

APPENDIX A: DESIGN OF COPLANAR WAVEGUIDE

In Fig. 5(a), the coplanar waveguide pattern employed for the measurements in the main text is illustrated. The wavelength λ and propagation gap d are 12 μm and 20 μm, respectively. Each waveguide consists of one signal line at the center and two ground lines at the both sides, which is terminated with a short circuit. When it is connected to the VNA through the GSG (ground-signal-ground) microprobe, the input current density for the signal and ground line is I_0^ν and $-I_0^\nu/2$, respectively. By taking the Fourier transform for the spatial distribution of current density $I^\nu(x)$, the wave-number distribution $|\tilde{I}^\nu(k)|^2$ can be estimated [31,32] as shown in Fig. 5(b). The main peak at $k_p = 0.50\ \mu\text{m}^{-1}$ satisfies the relationship $k_p \sim 2\pi/\lambda$, and its full width at half maximum (FWHM) is $\delta k = 0.37\ \mu\text{m}^{-1}$. The higher order peaks are also found for the larger k region, and the second largest one is at $k = 1.47\ \mu\text{m}^{-1}$ with the amplitude 1/7 times as small as that for the main peak. To simplify the discussion, we analyzed our ΔL_{nm} spectra assuming that the contribution from the main peak centered at k_p is dominant.

According to Eq. (4), the shift of spin wave frequency $\Delta\nu$ between $\pm k$ should be given by $\Delta\nu \propto D|k|$, as experimentally demonstrated in Fig. 4(b). To further confirm the k-linear nature of frequency shift, we also fabricated the linearly scaled waveguide pattern with $\lambda = 24\ \mu$m characterized by the peak wavelength at $k_p = 0.25\mu\text{m}^{-1}$ [Fig. 5(b)]. Figures 5(c) and 5(d) indicate the spectra of $|\Delta L_{21}|$ and $|\Delta L_{12}|$ measured at $H = 2H_c$ with the wave guides of $\lambda = 12\ \mu$m and $\lambda = 24\ \mu$m, respectively. Here, H_c represents the magnetic

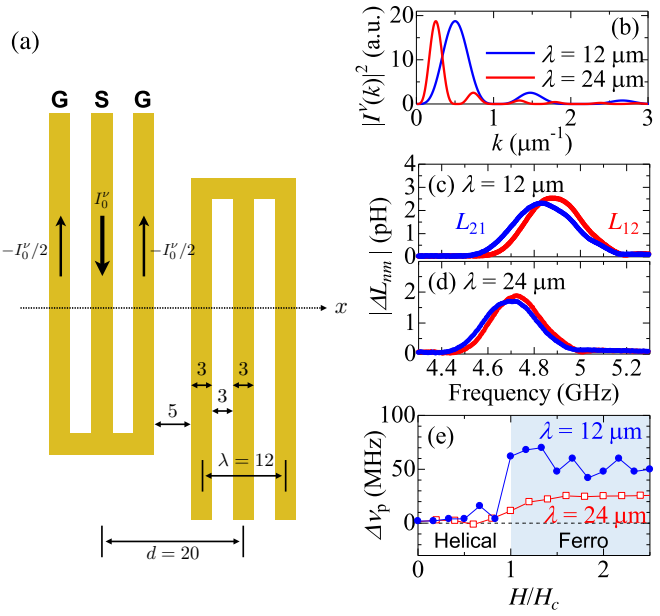

FIG. 5. (a) Schematic illustration of a pair of coplanar wave guides used for the spin wave spectroscopy. Each waveguide consists of one signal (S) line and two ground (G) lines. The associated current density distribution as well as length scale (in the unit of μm) are also shown. This wave-guide pattern with $\lambda = 12\ \mu$m has been employed for the measurements in the main text, while the linearly scaled pattern with $\lambda = 24\ \mu$m has also been used for the additional experiments. (b) The calculated wave-number distribution of excitation current for wave guides with different λ value. (c) and (d) The spectra of mutual inductance $|\Delta L_{12}|$ and $|\Delta L_{12}|$ at 30 K under $H = 2H_c$, measured with the wave guides of (c) $\lambda = 12\ \mu$m and (d) $\lambda = 24\ \mu$m. Here, H_c represents the critical magnetic field value necessary to induce the transition into the ferromagnetic state. (e) Magnetic field dependence of peak frequency shift $\Delta\nu_p$, obtained with the wave guides of different λ value.

field value necessary to induce the transition into the collinear ferromagnetic state. We found that the data obtained with $\lambda = 12\ \mu$m clearly shows larger magnitude of peak frequency shift $\Delta\nu_p$ than the one with $\lambda = 24\ \mu$m. In Fig. 5(e), we have plotted the magnetic field dependence of $\Delta\nu_p$ for each device. The averaged peak frequency shift in the collinear ferromagnetic state is $\Delta\nu_p \sim 50$ MHz for $\lambda = 12\ \mu$m and $\Delta\nu_p \sim 25$ MHz for $\lambda = 24\ \mu$m, consistent with the twice larger k_p value in the former case. This result strongly supports the $\Delta\nu \propto D|k|$ relationship in the present chiral-lattice ferromagnets, proving that the k-linear term of spin-wave dispersion caused by the DM interaction is the origin of observed nonreciprocity.

The wave-number distribution in wave guides [Fig. 5(b)] also affects the linewidth of ferromagnetic resonance. In Im$[\Delta L_{11}]$ spectrum, the FWHM $\delta\nu$ for the resonance peak at frequency ν_p can be given as [32]

$$\delta\nu = \frac{v_g^p \cdot \delta k}{2\pi} + 2\nu_p\alpha, \tag{A1}$$

with α representing the intrinsic Gilbert damping parameter. In the case of the present Cu_2OSeO_3 specimen at 740 Oe, $\delta\nu = 0.42$ GHz is obtained from the Im$[\Delta L_{11}]$ spectrum of Fig. 2(a) in the main text. Considering the corresponding

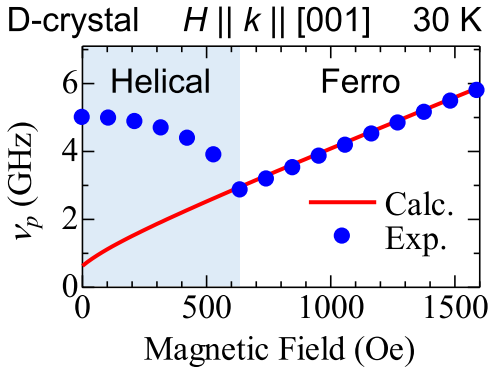

FIG. 6. Magnetic field dependence of resonance frequency ν_p in the ΔL_{21} spectrum, measured for the D crystal of Cu_2OSeO_3 at 30 K. The experimental data are taken from Fig. 3(a) in the main text, and the theoretical fit is by Eq. (4) in the main text with $k = k_p$.

averaged spin wave group velocity $v_g^p = 6.1$ km/s taken from Fig. 3(d) in the main text, the first term in Eq. (A1) gives ~ 0.36 GHz. This means that $\delta\nu$ mostly reflects the wave-number distribution associated with the wave-guide pattern. By using $\nu_p = 3.2$ GHz, we obtain the relatively small damping parameter $\alpha \sim 0.01$, which is consistent with the previous report [41]. This allows us to estimate the decay length of propagating spin wave $l_d = v_g^p/(2\pi\alpha\nu_p) = 30$ μm [32].

APPENDIX B: MATERIAL PARAMETERS

For Cu_2OSeO_3, the material parameters included in Eq. (4) in the main text can be estimated so as to reproduce the H dependence of magnetic resonance frequency ν_p in the ferromagnetic state (Fig. 6). In this process, several additional confinements are imposed [26]. The helical spin modulation period λ_h ($\sim$62 nm) [37,38] and the corresponding magnetic wave number $Q = 2\pi/\lambda_h$ in the ground state is given as

$$Q = -D/J, \tag{B1}$$

and the critical magnetic field $\mu_0 H_c$ ($\sim$0.063 T) satisfies

$$\frac{\gamma\hbar}{V_0}\mu_0 H_c = \frac{D^2 S}{J} - 2KS^3. \tag{B2}$$

The saturation magnetization is $M_s = \hbar\gamma S/V_0 = 0.46\mu_B/Cu^{2+}$ at 30 K, with $V_0 \sim 89$ Å^3 being the volume of formula unit cell of Cu_2OSeO_3. From these restrictions, we obtain $D = 3.4 \times 10^{-4}$ J/m^2, $J = 3.4 \times 10^{-12}$ J/m, $K = 6.9 \times 10^3$ J/m^3, $\gamma/2\pi = 29$ GHz T^{-1}, $\mu_0 M_s = 0.12$ T, and $S = 0.44$. These values are used to calculate the spin wave dispersion in Figs. 4(d) and 4(e) in the main text and H dependence of ν_p in Fig. 6. Similar values have also been reported in Ref. [41].

APPENDIX C: SYMMETRY OF SPIN CURRENT

Propagating spin wave can be considered as a kind of spin current (i.e., flow of magnetic moment) [18–20], which is generally characterized by the combination of wave vector $\vec{k}$ and carried magnetic moment $\vec{M}_0$. From the viewpoint of

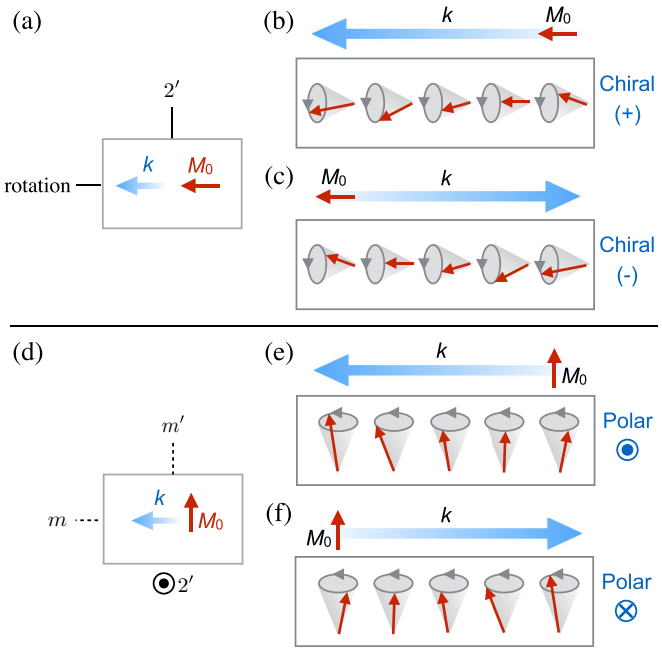

FIG. 7. Spin current (i.e., flow of magnetic moment) characterized by the wave vector $\vec{k}$ and the carried magnetic moment $\vec{M}_0$ under (a) $\vec{k} \parallel \vec{M}_0$ and (d) $\vec{k} \perp \vec{M}_0$ configurations. The compatible symmetry elements are also indicated, which reveals that the former and latter types of spin current belong to the chiral and polar symmetry, respectively. (b), (c), (e), and (f) Schematic illustration of spin wave spin current with various combinations of $\vec{k}$ and $\vec{M}_0$ for the uniform collinear ferromagnetic state. The red and gray arrows represent the directions of local magnetization and its precession, respectively. For each configuration, the application of space-inversion operation reverses $\vec{k}$ (but not $\vec{M}_0$), as well as the associated sign of the chirality or polarity of spin wave spin current.

the symmetry, there are two types of spin wave spin current (SWSC) for ferromagnets, depending on the directional relationship between $\vec{M}_0$ ($\parallel \vec{H}$) and $\vec{k}$. In case of $\vec{k} \parallel \vec{M}_0$ [Figs. 7(a) and 7(b)], the SWSC doesn't have any mirror plane or space-inversion center and belongs to the chiral symmetry [11]. In contrast, the SWSC with $\vec{k} \perp \vec{M}_0$ configuration [Figs. 7(d) and 7(e)] has the polar symmetry with the polar axis normal to both $\vec{M}_0$ and $\vec{k}$. For each case, the reversal of $\vec{k}$ gives the SWSC with opposite chirality or polarity [Figs. 7(c) and 7(f)].

The above analysis predicts that the SWSCs propagating along the positive and negative direction can show different propagation characters, when placed in the chiral or polar environment depending on the symmetry of SWSC. For example, the surface (or interface) is always characterized by the structural polarization normal to the surface. When both $\vec{k}$ and $\vec{M}_0$($\parallel \vec{H}$) are confined within the surface plane keeping the $\vec{k} \perp \vec{M}_0$ relationship, the polar axis of SWSC [Figs. 7(b) and 7(c)] becomes parallel or antiparallel to the polarization of the surface and thus the asymmetric spin wave propagation between $\pm k$ can be expected. Such a surface-induced spin wave nonreciprocity was predicted by Damon and Eshbach [22] and then verified by various experimental techniques such as spin wave spectroscopy [23,57], spin-polarized electron energy loss spectroscopy [53],

thermography [56], and Brillouin light scattering [54,55]. In particular, the $k \to 0$ mode mediated by the magnetic dipole-dipole interaction in this $\vec{k} \perp \vec{M}_0$ configuration is called magnetostatic surface spin wave (representing that it can propagate only at the surface of the sample) and is known for its unidirectional propagation character [22–24]. Nevertheless, such a surface-driven nonreciprocity can cancel out as the entire sample, since the sign of structural polarity (and the resultant nonreciprocity of surface spin wave) is generally opposite between the top and bottom surfaces [56]. While the application of spatially inhomogeneous excitation field can partly avoid this cancellation, an alternative approach providing uniform nonreciprocity independent of the surface polarity is highly demanded.

In contrast, the $k \to 0$ mode in the $\vec{k} \parallel \vec{M}_0$ configuration as investigated in this study is called magnetostatic volume spin wave, which is known to propagate through the entire volume of the sample [23]. While the volume spin wave mode doesn't show any nonreciprocity in the centrosymmetric materials [22,24], the chiral symmetry of this mode [Figs. 7(b) and 7(c)] implies its nonreciprocal propagation character in materials with chiral crystallographic lattice. Since this idea involves the symmetry breaking by the bulk crystallographic lattice (rather than the surface), we can expect uniform rectification function throughout a single-component crystal. In this study, we have examined such a nonreciprocal propagation nature of volume spin wave for a chiral-lattice ferromagnet Cu_2OSeO_3 in terms of spin wave spectroscopy.

[1] L. D. Barron, Nature (London) **405**, 895 (2000).
[2] G. L. J. A. Rikken, Science **331**, 864 (2011).
[3] A. Fert, V. Cros, and J. Sampaio, Nat. Nanotechnol. **8**, 152 (2013).
[4] N. Nagaosa and Y. Tokura, Nat. Nanotechnol. **8**, 899 (2013).
[5] S. Seki and M. Mochizuki, *Skyrmions in Magnetic Materials* (Springer, New York, 2015).
[6] U. K. Rößler, A. N. Bogdanov, and C. Pfleiderer, Nature (London) **442**, 797 (2006).
[7] S. Mühlbauer, B. Binz, F. Jonietz, C. Pfleiderer, A. Rosch, A. Neubauer, R. Georgii, and P. Böni, Science **323**, 915 (2009).
[8] X. Z. Yu, Y. Onose, N. Kanazawa, J. H. Park, J. H. Han, Y. Matsui, N. Nagaosa, and Y. Tokura, Nature (London) **465**, 901 (2010).
[9] K. Shibata, X. Z. Yu, T. Hara, D. Morikawa, N. Kanazawa, K. Kimoto, S. Ishiwata, Y. Matsui, and Y. Tokura, Nat. Nanotechnol. **8**, 723 (2013).
[10] L. D. Barron and J. Vrbancich, Molec. Phys. **51**, 715 (1984).
[11] L. D. Barron, J. Am. Chem. Soc. **108**, 5539 (1986).
[12] G. L. J. A. Rikken, E. Raupach, Nature (London) **390**, 493 (1997).
[13] C. Train, R. Gheorghe, V. Krstic, L. M. Chamoreau, N. S. Ovanessyan, G. L. J. A. Rikken, M. Gruselle, and M. Verdaguer, Nat. Mater. **7**, 729 (2008).
[14] S. Kibayashi, Y. Takahashi, S. Seki, and Y. Tokura, Nat. Commun. **5**, 4583 (2014).
[15] Y. Okamura, F. Kagawa, S. Seki, M. Kubota, M. Kawasaki, and Y. Tokura, Phys. Rev. Lett. **114**, 197202 (2015).
[16] G. L. J. A. Rikken, J. Fölling, and P. Wyder, Phys. Rev. Lett. **87**, 236602 (2001).
[17] F. Pop, P. Auban-Senzier, E. Canadell, G. L. J. A. Rikken, and N. Avarvari, Nat. Commun. **5**, 3757 (2014).
[18] S. Maekawa, S. O. Valenzuela, E. Saitoh, and T. Kimura, *Spin Current* (Oxford University Press, Oxford, 2012).
[19] Y. Kajiwara, K. Harii, S. Takahashi, J. Ohe, K. Uchida, M. Mizuguchi, H. Umezawa, H. Kawai, K. Ando, K. Takanashi, S. Maekawa, and E. Saitoh, Nature (London) **464**, 262 (2010).
[20] K. Uchida, J. Xiao, H. Adachi, J. Ohe, S. Takahashi, J. Ieda, T. Ota, Y. Kajiwara, H. Umezawa, H. Kawai, G. E. W. Bauer, S. Maekawa, and E. Saitoh, Nat. Mater. **9**, 894 (2010).
[21] S. Murakami, N. Nagaosa, and S. C. Zhang, Science **301**, 1348 (2003).
[22] R. W. Damon and J. R. Eshbach, J. Phys. Chem. Solids **19**, 308 (1961).
[23] D. D. Stencil, *Theory of Magnetostatic Waves* (Springer, New York, 1993).
[24] A. G. Gurevich and G. A. Melkov, *Magnetization Oscillations and Waves* (CRC Press, New York, 1996).
[25] P. Bak and M. H. Jensen, J. Phys. C **13**, L881 (1980).
[26] M. Kataoka, J. Phys. Soc. Jpn. **56**, 3635 (1987).
[27] D. Cortés-Ortuño and P. Landeros, J. Phys.: Condens. Matter **25**, 156001 (2013).
[28] Y. Ishikawa, G. Shirane, J. A. Tarvin, and M. Kohgi, Phys. Rev. B **16**, 4956 (1977).
[29] P. Y. Portnichenko, J. Romhanyi, Y. A. Onykiienko, A. Henschel, M. Schmidt, A. S. Cameron, M. A. Surmach, J. A. Lim, J. T. Park, A. Schneidewind, D. L. Abernathy, H. Rosner, Jeroen van den Brink, and D. S. Inosov, Nat. Commun. **7**, 10725 (2016).
[30] Y. Iguchi, S. Uemura, K. Ueno, and Y. Onose, Phys. Rev. B **92**, 184419 (2015).
[31] V. Vlaminck and M. Bailleul, Science **322**, 410 (2008).
[32] V. Vlaminck and M. Bailleul, Phys. Rev. B **81**, 014425 (2010).
[33] H. Effenberger and F. Pertlik, Monatsch. Chem. **117**, 887 (1986).
[34] J.-W. G. Bos, C. V. Colin, and T. T. M. Palstra, Phys. Rev. B **78**, 094416 (2008).
[35] K. Kohn, J. Phys. Soc. Jpn. **42**, 2065 (1977).
[36] S. Seki, X. Z. Yu, S. Ishiwata, and Y. Tokura, Science **336**, 198 (2012).
[37] S. Seki, J.-H. Kim, D. S. Inosov, R. Georgii, B. Keimer, S. Ishiwata, and Y. Tokura, Phys. Rev. B **85**, 220406 (2012).
[38] T. Adams, A. Chacon, M. Wagner, A. Bauer, G. Brandl, B. Pedersen, H. Berger, P. Lemmens, and C. Pfleiderer, Phys. Rev. Lett. **108**, 237204 (2012).
[39] K. H. Miller, X. S. Xu., H. Berger, E. S. Knowles, D. J. Arenas, M. W. Meisel, and D. B. Tanner, Phys. Rev. B **82**, 144107 (2010).
[40] Y. Onose, Y. Okamura, S. Seki, S. Ishiwata, and Y. Tokura, Phys. Rev. Lett. **109**, 037603 (2012).
[41] T. Schwarze, J. Waizner, M. Garst, A. Bauer, I. Stasinopoulos, H. Berger, C. Pfleiderer, and D. Grundler, Nat. Mater. **14**, 478 (2015).
[42] Y. Okamura, F. Kagawa, M. Mochizuki, M. Kubota, S. Seki, S. Ishiwata, M. Kawasaki, Y. Onose, and Y. Tokura, Nat. Commun. **4**, 2391 (2013).

[43] C. Vittoria, Phys. Rev. B **92**, 064407 (2015).
[44] S. V. Grigoriev, D. Chernyshov, V. A. Dyadkin, V. Dmitriev, E. V. Moskvin, D. Lamago, Th. Wolf, D. Menzel, J. Schoenes, S. V. Maleyev, and H. Eckerlebe, Phys. Rev. B **81**, 012408 (2010).
[45] V. Dyadkin, K. Prsa, S. V. Grigoriev, J. S. White, P. Huang, H. M. Ronnow, A. Magrez, C. D. Dewhurst, and D. Chernyshov, Phys. Rev. B **89**, 140409(R) (2014).
[46] T. Moriya, Phys. Rev. **120**, 91 (1960).
[47] D. Belitz, T. R. Kirkpatrick, and A. Rosch, Phys. Rev. B **73**, 054431 (2006).
[48] M. Janoschek, F. Bernlochner, S. Dunsiger, C. Pfleiderer, P. Böni, B. Roessli, P. Link, and A. Rosch, Phys. Rev. B **81**, 214436 (2010).
[49] C. Vittoria and N. D. Wilsey, J. Appl. Phys. **45**, 414 (1974).
[50] A. T. Costa, R. B. Muniz, S. Lounis, A. B. Klautau, and D. L. Mills, Phys. Rev. B **82**, 014428 (2010).
[51] J.-H. Moon, S.-M. Seo, K.-J. Lee, K.-W. Kim, J. Ryu, H.-W. Lee, R. D. McMichael, and M. D. Stiles, Phys. Rev. B **88**, 184404 (2013).
[52] L. Udvardi and L. Szunyogh, Phys. Rev. Lett. **102**, 207204 (2009).
[53] Kh. Zakeri, Y. Zhang, J. Prokop, T.-H. Chuang, N. Sakr, W. X. Tang, and J. Kirschner, Phys. Rev. Lett. **104**, 137203 (2010).
[54] K. Di, V. L. Zhang, H. S. Lim, S. C. Ng, M. H. Kuok, J. Yu, J. Yoon, X. Qiu, and H. Yang, Phys. Rev. Lett. **114**, 047201 (2015).
[55] J. Cho, N.-H. Kim, S. Lee, J.-S. Kim, R. Lavrijsen, A. Solignac, Y. Yin, D.-S. Han, N. J. J. van Hoof, H. J. M. Swagten, B. Koopmans, and C.-Y. You, Nat. Commun. **6**, 7635 (2015).
[56] T. An, V. I. Vasyuchka, K. Uchida, A. V. Chumak, K. Yamaguchi, K. Harii, J. Ohe, M. B. Jungfleisch, Y. Kajiwara, H. Adachi, B. Hillebrands, S. Maekawa, and E. Saitoh, Nat. Mater. **12**, 549 (2013).
[57] L. K. Brundle and N. J. Freedman, Electron. Lett. **4**, 132 (1968).